

# Numerical Analysis of Boiling Coolant in Reciprocating Compressor Cylinderhead

<sup>1</sup>M. Kiszely, <sup>1</sup>Á. Veress, <sup>1</sup>G. Holler <sup>2</sup>L. Palkovics

<sup>1</sup>Széchenyi István University, H-9026, Győr, Egyetem tér 1.

e-mail: [kiszely.marcell@gmail.com](mailto:kiszely.marcell@gmail.com), [veress@freemail.hu](mailto:veress@freemail.hu) and [holler66@yahoo.com](mailto:holler66@yahoo.com)

<sup>2</sup>Budapest University of Technology and Economics, H-1111, Bp., Sztoczek u. 6. J ép. V. emelet, e-mail: [palko@auto.bme.hu](mailto:palko@auto.bme.hu)

**Abstract:** Thermal interaction of fluid and solid is investigated utilizing steady state Computational Fluid Dynamics (CFD) model. Beyond the capability of modelling single phase flow, the factors that initialize boiling phenomena and affect its intensity are also studied and implemented. An alternative of modelling fluid behaviour under circumstances where this thermal phase change can occur is introduced. The herein presented method highlights the practical usage of fluid flow modelling.

**Keywords:** *CFD, coolant, boiling*

## 1. Introduction

The increasing computational resources makes virtual modelling and analysis possible to be used expansively in engineering practise involving models that can cover more and more complex physical phenomena. CFD is one of the most effective and developing simulation tool, which is commonly used in Computer Aided Engineering (CAE). Software developer companies put an intensive effort to implement novel sub-models based on state-of-the-art research results in order to further expand the broad scale of flow types for that simulation is getting available.

Inadequate cooling of machines can lead to subsequent malfunction of many sorts; hence analysing fluid behaviour has extraordinary importance when designing for example a cylinderhead. Despite the mechanical and sealing restrictions, designers need to take extra care of ideal coolant volume shape as this plays a significant role in overall cooling effectiveness. CFD provides a feasible method for checking design accuracy in terms of the mentioned aspect. Instead of manufacturing a series of prototypes and testing them on bench, conceptual dead-ends can be easily excluded by executing relatively cheap and fast simulations. It is mandatory therefore, to develop a simulation model that gives acceptable result for any required environmental condition.

## 2. Investigated model description

In the focus of this work, the thermal interaction of fluid and solid is modelled regarding the water jacket inside a reciprocating compressor's cylinderhead. Elevated thermal

environment surrounding this coolant can cause such high wall temperature on the bounding surfaces of fluid region that may results in phase change. Thermal phase change (boiling) enhances heat transfer, so exposing the build up of this phenomenon and the parameters that drive its intensity are also the aim of this study.

The device under investigation is a reciprocating compressor with two bores and cooled cylinderhead. Fluid circulates inside the assembly in a single channel that crosses main metal parts. As it can be noticed in *Figure 1*, the cylinderhead is built up in a layered manner consisting of aluminium and cast iron parts. The investigated part is the lowermost (heat critical) layer coloured dark grey.

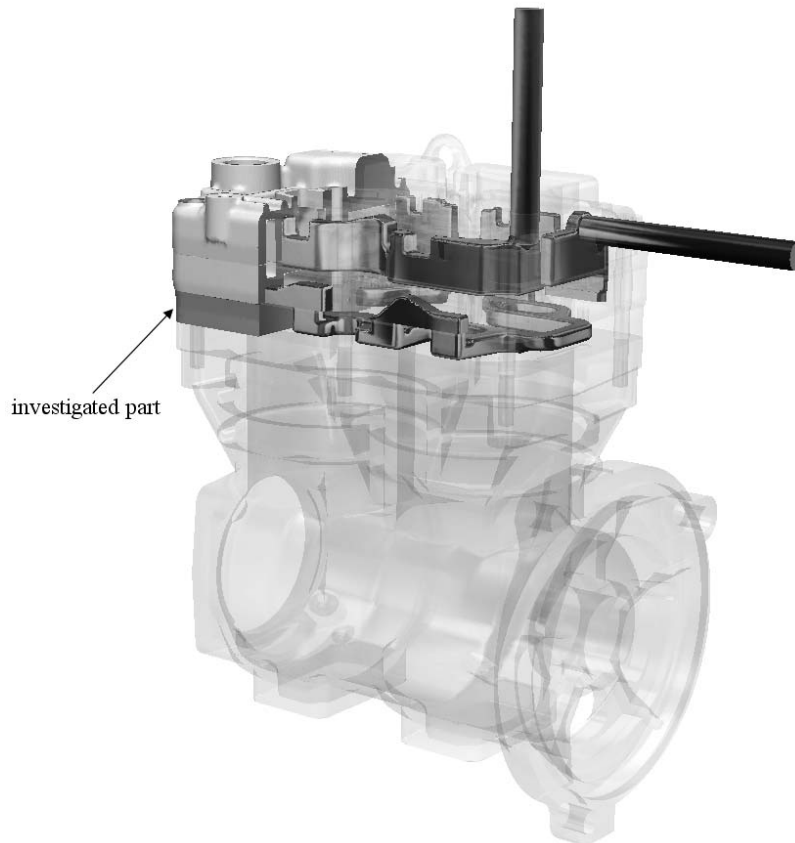


*Figure 1. Reciprocating compressor cylinderhead with inner water jacket (The faded crankcase is not a part of the simulation model; its presence in the pictures serves for interpretation only)*

When the compressor is in operation, air is compressed inside the cylinders and squeezed through exhaust valves and ports towards the reservoir via pipes. During this process hot air heats up the entire cylinderhead that can cause increased evaporation of oil in the crankcase. This parasitic vapour could lead to further damage in the system as it can create coke depositions in the exhaust channels and inside the air filter cartridge.

Therefore, it is the coolant that supposed to extract heat from metal surfaces of the cylinderhead to keep temperature at a reasonable level. An ideal case would be a water jacket that has higher velocity values where the thermal load is higher and lower value where less cooling is adequate. Of course, due to the accommodation to other requirements with even higher priority such shape can hardly be created. After determining the most crucial locations to be intensively cooled, flow path should be shaped by designers so that continuous flow is maintained at these regions. As fluid velocity is in very close relation to convective heat transfer, acquiring its pattern can show any imperfection in terms of cooling capabilities. Besides flow characteristics, CFD makes the complete thermal mapping available for both fluid and solid materials within the system. With investigating wall temperatures along with fluid velocity in the vicinity, further hazardous locations can be discovered, while temperature differences of solid parts are also useful for heat expansion calculations.

### 3. The boiling phenomena

In addition to the upper described benefits of modelling a continuous fluid, including a thermal phase change model can provide further useful information on flow behaviour. Note that every statement and graph herein that concern boiling refer to the thermal phase change of pure water. Two types of boiling can be distinguished in terms of its occurrence: boiling in natural convection (pool boiling) and boiling in forced convection. Generally, phase change from water to steam initiated when the fluid temperature reaches and exceeds its saturation temperature. Pool boiling has been intensively inspected and measured in the past. It is observed in test-bench experiments that multiple modes of boiling can be determined. The *Figure 2* shows these individual regimes that occur during pool boiling of water at atmospheric pressure. The heat flux  $\dot{q}_w$  is plotted as a function of the wall superheat  $\Delta T_w = T_w - T_{sat}$  on a log-log scale [1].

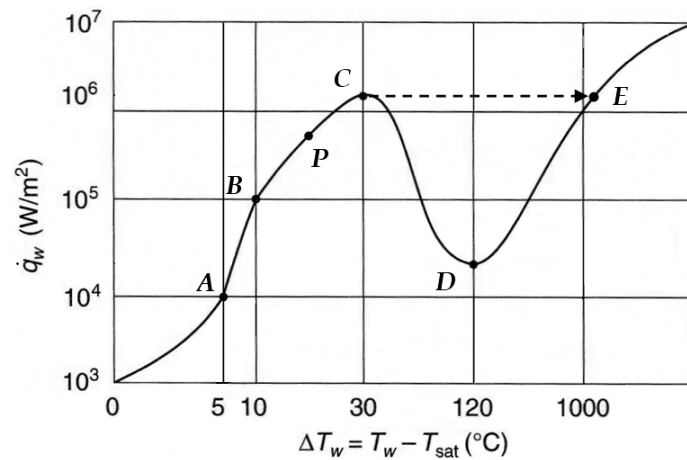


Figure 2. Typical boiling curve for water (N-curve) [1]

In the range of *ABC* the curve represents the developed *nucleate boiling*, *CD* range refers to *partial film boiling*, while the final ascending branch of the boiling curve (*DE*) is characterized as the region of *film boiling*. Similar trends have been observed for other fluids. The importance of critical heat flux point (*C*) is obvious. In many applications such as in a boiler of a power plant, the boiling is  $\dot{q}_w$ -controlled. In these cases the transition from point *C* to point *E* can be very rapid. The wall temperature that belongs to point *E* is so high that it may exceed the melting point of the material. For this reason, point *C* is often termed as *burnout point*. When designing devices with coolant circuit, an engineer may want to operate the equipment close to this value, but would never risk exceeding it [1]. Therefore, the limit of *nucleate boiling* range is getting higher importance when setting up a model for analysis.

Focusing on this boiling mode, it is necessary to run through the parameters that characterize its bubbling process. Figure 3 depicts the interrelationship of them, abstracted in four levels.

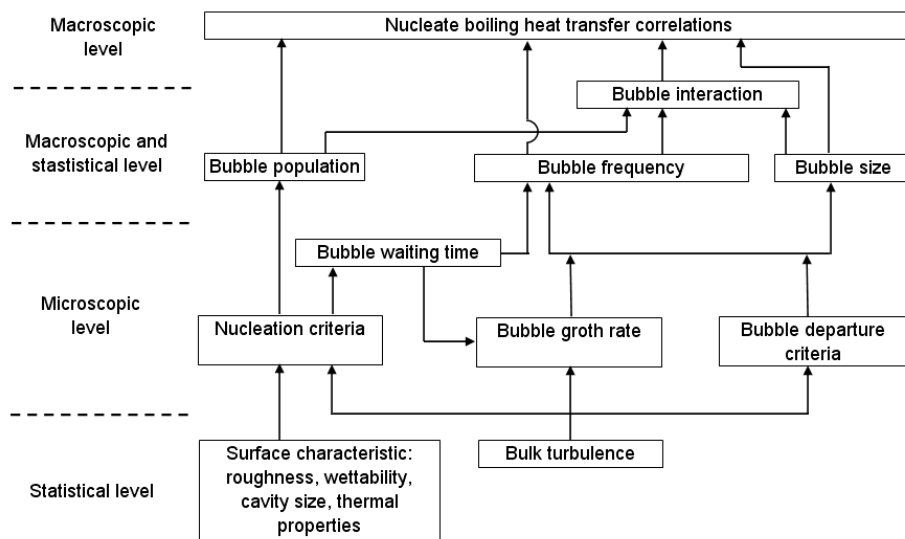


Figure 3. The interrelationship of the bubbling process parameters [2]

The parameters and the relations in-between are hard to analytically express, although many of them have already been studied in detail by [2], [3] and [4]. The recent numerical study utilizes CFX 13.0 solver from ANSYS. Some of the mentioned parameters are already implemented into the code and are available as: “Wall nucleation site density”, “Area influence factors”, “Bubble departure diameter”, “Bubble detachment frequency”. The sub-model add-ons are characterized to be adequate for both natural and forced convection type of boiling. Due to the bulk motion of coolant in a cylinderhead, the inspection of forced convection boiling process is of higher relevance.

Whereas the intensity of heat transfer in pool boiling is mainly governed by the difference of saturation and wall temperatures, material and surface properties, in case

of a moving fluid, the increased number of forces that are acting on steam bubbles (inertial, excess pressure, lift and drag) also plays a significant role. If at the same location, the temperature of bulk fluid remains below saturation, the boiling process is known as subcooled boiling flow. This type of boiling is usually characterized by a high-temperature two-phase region near the heated wall and a low-temperature single-phase liquid away from the heated surface. Two phase flow pattern in heated pipes show similarity for vertical and horizontal alignments. The higher the mass flow rate, the more similarity is observed.

Typical forms of boiling can be traced in *Figure 4*, where the void fraction is growing streamwise from zero to 100%. The terms of certain forms are also assigned for both pipe alignments.

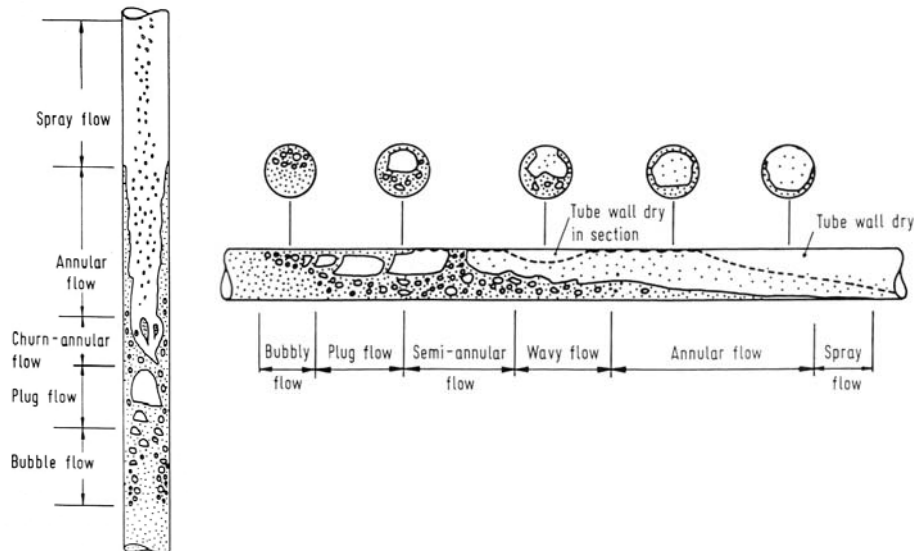


Figure 4. Two phase flow patterns in heated vertical and horizontal pipes [4]

#### 4. Simulation pre-processing

The CFD simulation is based on a steady state Reynolds-Averaged Navier-Stokes (RANS) model with two-equation turbulence approximation ( $k-\omega$ ), continuity and energy equations all solved for each phase. Two phases are defined: incompressible water (liquid) and compressible steam (gaseous). In addition to a single phase fluid modelling, the herein presented method involves the thermal phase change mass transfer module that makes the simulation of steam propagation possible.

##### 4.1. Boundary conditions

Mass flow inlet boundary type is paired with static outlet pressure. The reference pressure is 6 bar, while inlet mass is 243 g/s (100% liquid phase). Constant temperature boundaries are also applied to certain solid surfaces representing heat sources (wall

temperature of bores and crankcase, while ambient condition is assumed for outer surfaces with  $8 \text{ W/m}^2\text{K}$  heat transfer coefficient and  $25^\circ\text{C}$  temperature.

#### 4.2. Material properties

The pressure of coolant in a commercial vehicle's engine varies in between 1.2 and 2.5 bar (absolute values) depending on engine RPM (from idle to maximum). This pressure range is valid for a continuous fluid at  $90^\circ\text{C}$ . If the temperature is raising and the fraction of steam phase is increasing, the thermal expansion of gaseous volume can further increase system pressure, which has feedback on water saturation. The higher the system pressure, the higher the saturation temperature. Consequently, in order to model local void propagation, the material properties of coolant should be able to follow this dependency (see *Figure 5*).

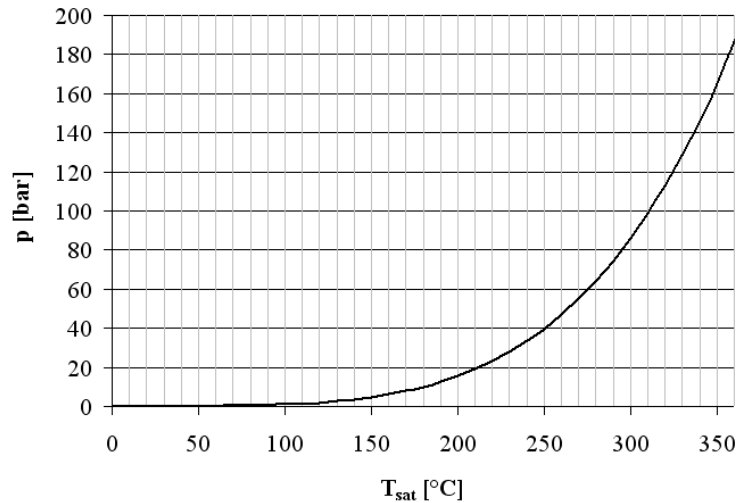


Figure 5. Water saturation  $p$ - $T$  curve [9]

The saturation curve is manually added to the code, while the basic properties of water and steam are set according to the IAPWS<sup>1</sup> database.

#### 4.3. Numerical mesh

Spatial discretization requires a further statement that is of high importance. ANSYS has implemented a 1-D wall boiling model in 3-D so that the results are nearly mesh independent for  $30 < y^+ < 300$  range<sup>2</sup>. This has been tested, for example, on the Bartolomej test case. However, it is found that a smaller  $y^+$  can prevent convergence in some cases. This is caused by the large rate of production of vapour in the first cell of the mesh immediately next to the wall. This will be corrected in future software releases by distributing the vapour over a region near the wall that has the thickness of the

<sup>1</sup> The International Association for the Properties of Water and Steam.

<sup>2</sup>  $y^+$  is a non-dimensional measure of distance from wall. Its value mainly depends on the geometrical thickness of first mesh layer (considering constant velocity).

bubble departure diameter. Meanwhile it is advised to avoid using  $y^+ < 30$ , especially for cases with high heat fluxes [5]. As this non-dimensional value is a result that could only be evaluated after simulation was completed, initial calculations are required in order to set correct mesh size (see Figure 6.).

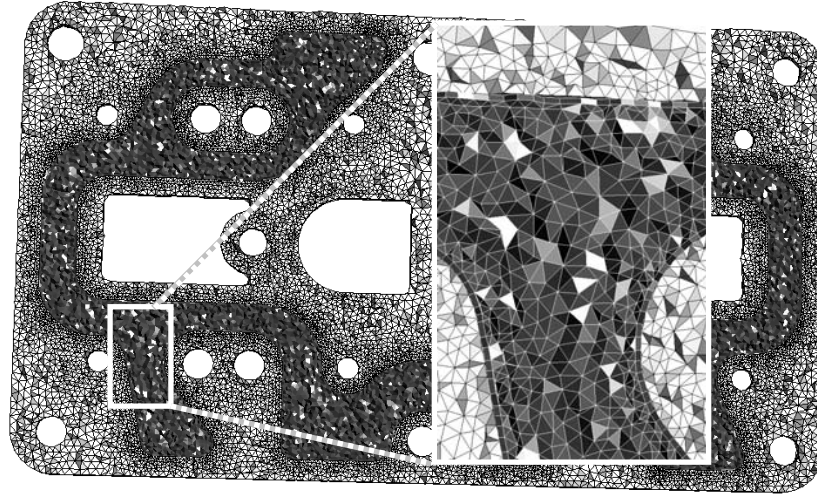


Figure 6. Applied numerical mesh on solid (light grey) and fluid (dark grey) domains (median section of lowermost part; note the lack of boundary layer refinement to maintain the advised  $30 < y^+ < 300$  condition in fluid)

#### 4.4. Mesh sensitivity

In order to check how sensitive the results are to fluid domain resolution, three mesh variants are generated with different volume cell density. For this investigation a simplified model is set up with single water phase and constant heat flux on the walls (solids are not modelled). Boundary layer thickness is identical at all cases. Outlet temperature change is seen in Figure 7.

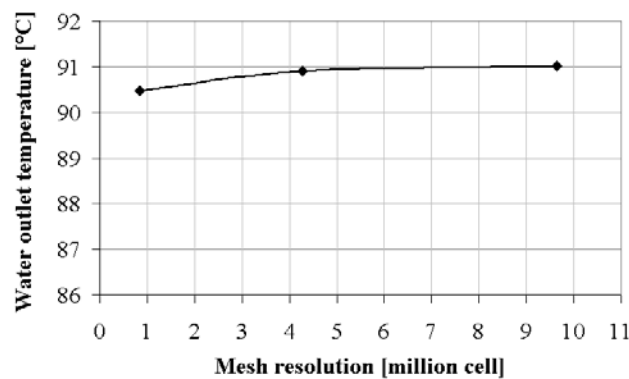


Figure 7. Mesh sensitivity

It is observed that variation of outlet temperature is less than 1%, hence the optimal resolution for further analysis is in the range of 1-4 million cells in fluid domain. Considering computational time and ideal transition in volume size of boundary layer prismatic and adjacent tetrahedral elements, the second variant is selected (4.3 million cells) for boiling phenomena modelling.

## 5. Modelling boiling

The wall boiling model utilized within the CFD solver is based on the work of Kurul and Podowsky [6] and is called Rensselaer Polytechnic Institute (RPI) nucleate boiling model [8]. According to the basic RPI model, the total heat flux from the wall to the liquid is partitioned into three components, namely the convective heat flux ( $\dot{q}_C$ ), the quenching heat flux ( $\dot{q}_Q$ ) and the evaporative heat flux ( $\dot{q}_E$ ) (subscripts: *l*-liquid, *v*-vapour, *W*-wall, *b*-bubble):

$$\dot{q}_W = \dot{q}_C + \dot{q}_Q + \dot{q}_E \quad (1)$$

$$\dot{q}_C = h_C (T_W - T_l) (1 - A_b) \quad (2)$$

$$\dot{q}_Q = \frac{2k_l}{\sqrt{\pi\lambda_l T}} (T_W - T_l) \quad (3)$$

$$\dot{q}_E = V_b N_W \rho_v h_{lv} f \quad (4)$$

In the expression of quenching heat flux,  $\lambda_l = \frac{k_l}{\rho_l C_{pl}}$  is the diffusivity (where  $k_l$  is the thermal conductivity of fluid) and  $T$  is the periodic time of bubble departure.

As it is prefaced earlier, the various components of RPI boiling model feature sub-models that improve simulation accuracy. These are as follows:

### 5.1. Wall nucleation site density

Referring to the statistical level of bubbling process scheme, the nucleation site density is approximated through an area factor in convective (2) and directly in evaporative (4) heat flux terms with the empirical expression of

$$N_W = C^n (T_W - T_{sat})^n \quad (5)$$

according to the work of Lemmert and Chawla [7], with  $C = 210$  and  $n = 1.805$  constants.

### 5.2. Area of influence

Convective heat flux is expressed in equation (2), where  $h_C$  is the single phase heat transfer coefficient,  $T_W$  and  $T_l$  are the wall and liquid temperatures, respectively. Within this formula  $A_b$  refers to the size of solid surface, which is in touch with vapour



bubbles. It is not a real surface area, rather a non dimensional factor. In order to avoid numerical instabilities due to unbound empirical correlations for the nucleate site density, the area of influence has to be restricted. The area of influence is limited as follows:

$$A_b = \min \left( 1, K \frac{N_W \pi D_W^2}{4} \right) \quad (6)$$

The value of the empirical constant  $K$  is usually set to 4, however it has been found that this value is not universal and may vary between 1.8 and 5 [8].

### 5.3. Bubble departure frequency

Researchers found that for expressing evaporation rate, it is necessary to define the frequency of bubble detachment from nucleation site [8].

$$f = \frac{1}{T} = \sqrt{\frac{4g(\rho_l - \rho_v)}{3\rho_l D_W}} \quad (7)$$

### 5.4. Bubble departure diameter

The model calculates an instantaneous diameter for bubbles for departure according to Kurul and Podowsky [6]:

$$D_W = \min \left( D_{ref} e^{\frac{T_W - T_l}{\Delta T_{ref}}}; D_{max} \right) \quad (8)$$

Where the reference diameter is  $D_{ref} = 0.6$  mm, maximum diameter is  $D_{max} = 1.4$  mm and reference temperature difference is  $\Delta T_{ref} = 45$  K.

## 6. Results

The boundary condition that mainly contributes to the temperature level of the entire assembly is the one refers to the temperature inside the compressor's cylinders. This first-type boundary is set according to pre-calculations utilizing bore diameter, stroke, compression and mass flow:  $T_{bore} = 220^\circ\text{C}$ . It is observed, that the thermal load on the lowermost part of the cylinderhead (dark coloured part in *Figure 1*) is of one magnitude higher than on the two others above it. The most critical region in terms of thermal load to the structure occurs, where high temperature gradient pairs with relatively thin metal casing. For these reasons, the part that is directly exposed to bore temperature is selected for thermal inspections.

### 6.1. Solution convergence

The initial conditions were assuming stagnant flow at  $T_{init} = 86^\circ\text{C}$ ,  $p_{init} = 6$  bar with zero fraction of vapour phase. The numerical solution of the system of equations is

maintained after  $\sim 900$  iterations. The convergence history for equations' root mean square (RMS) residuals can be traced in *Figure 8*.

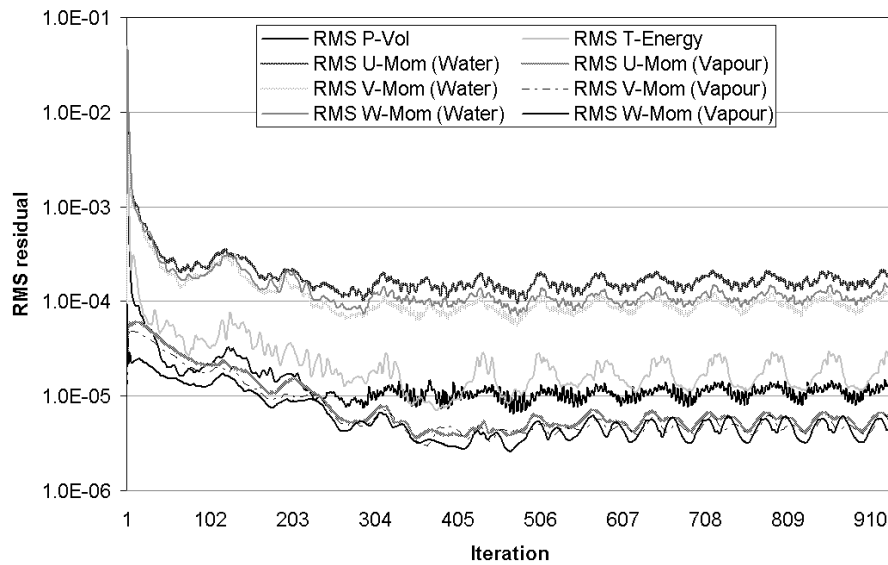


*Figure 8. Qualitative convergence history*

In addition to qualitatively tracing the residuals through the iterations, it is also advised to plot and observe specific physical values. In this case, the temperature of outflow is monitored, as well as the integral of heat flux that evolves on the surfaces of the upper selected part being in contact with fluid domain (*Figure 9*). While the former convergence indicator is “the lower, the better”, this second type helps to visualize, whether a steady state condition of a property is indeed reached.

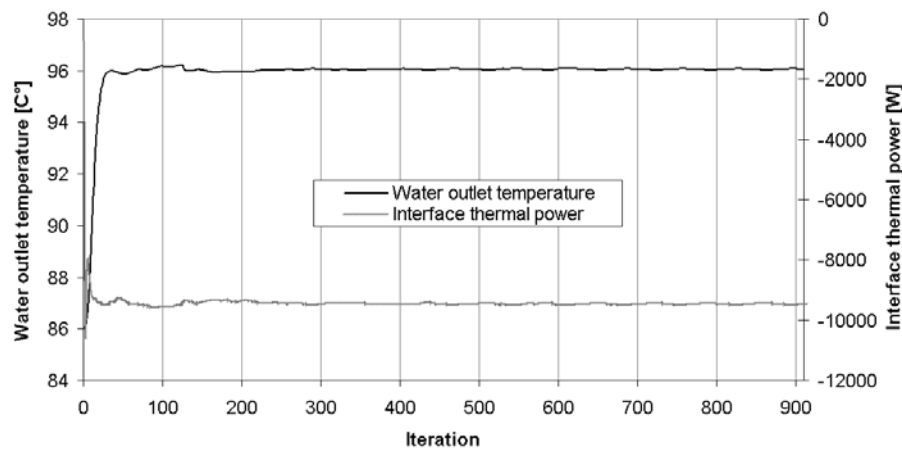


*Figure 9. Quantitative convergence history*

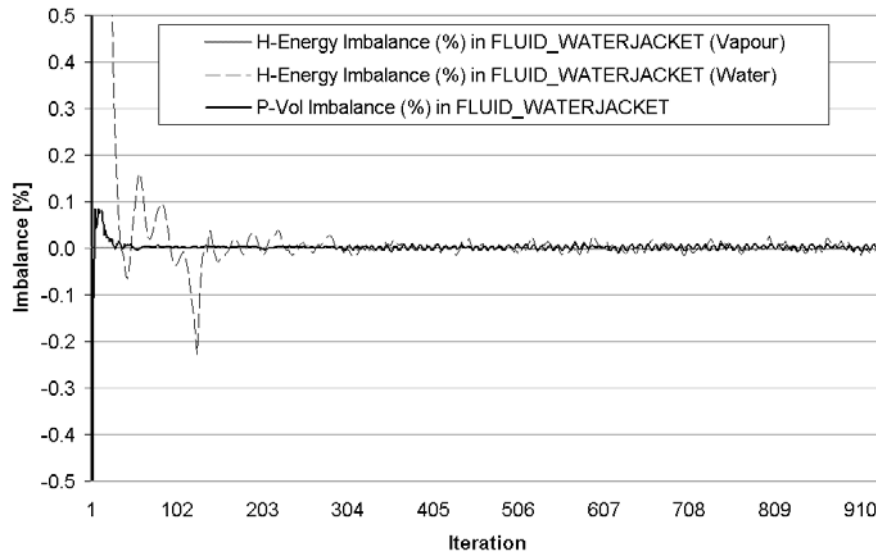


Figure 10. Energy and volume imbalance convergence history

The imbalances represent the actual residuals of the conservation laws – in linearized and discretized form – for the entire computational domain (Figure 10.). The convergence history for the pressure and enthalpy imbalances shows that the simulation is converged after around 400 iterations.

All of the convergence monitor types show negligible changes with further iterations, so the result represents a steady state, converged solution.

## 6.2. Representation of the result

Initially, the value of  $y^+$  should be checked. As it can be noticed in Figure 11, due to the applied boundary layer mesh size, the value of  $y^+$  is mostly within  $30 < y^+ < 300$  range on solid surfaces.

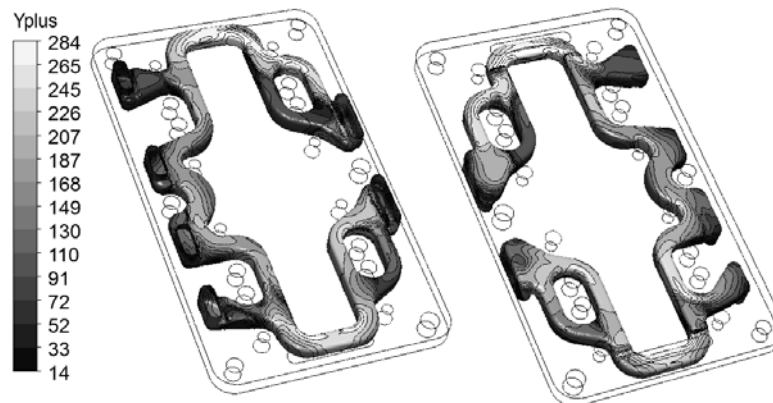
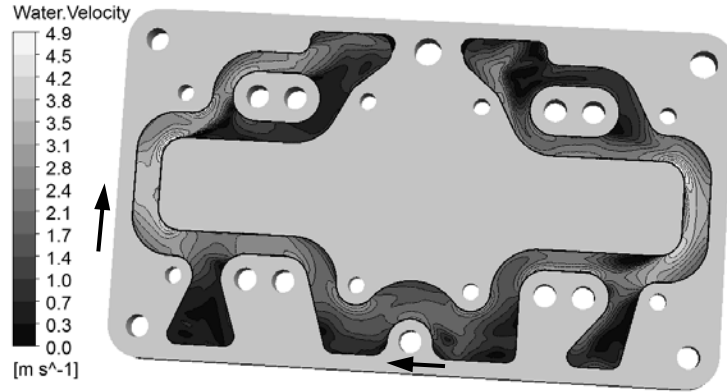


Figure 11. Distribution of  $y^+$  on boiling critical walls (top and bottom views)

One of the most informative quantities to describe a flow field is local fluid velocity. Its pattern at various sections can give an insight to overall fluid behaviour and even simulation plausibility.

In this case the bulk component of the fluid is incompressible viscous water. Primary flow direction and velocity distribution of water is shown in *Figure 12*. Note the stagnant zones where velocity is below  $0.3 \text{ m/s}$ .



*Figure 12. Velocity distribution of the coolant on median section plane*

The saturation temperature of water is  $T_{sat} \cong 165^\circ\text{C}$  in case the pressure is 6 bar. Solid surfaces exceeding this temperature are possible locations for *nucleate boiling*. A contour plot of solid temperature is seen in *Figure 13*. This distribution is a result of energy equilibrium between coolant and contacting metal part (temperature of fluid and solid domains on their interfaces are equal).

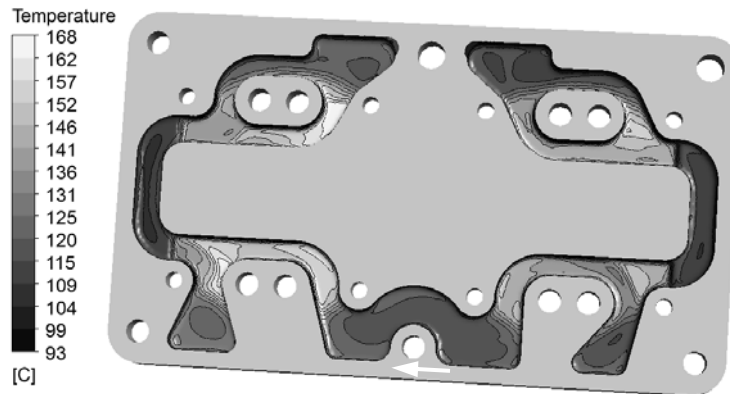


*Figure 13. Temperature distribution on solid surfaces being in contact with fluid*

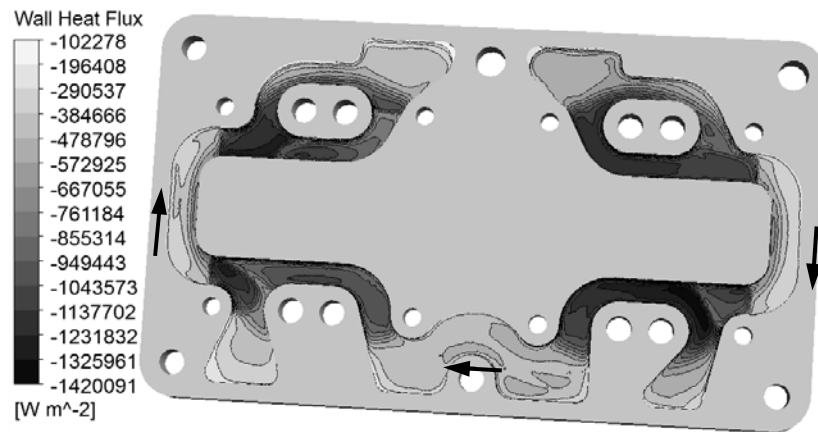


Figure 14. Heat flux distribution on solid surfaces being in contact with fluid (negative value refers to heat transferred from solid to fluid)

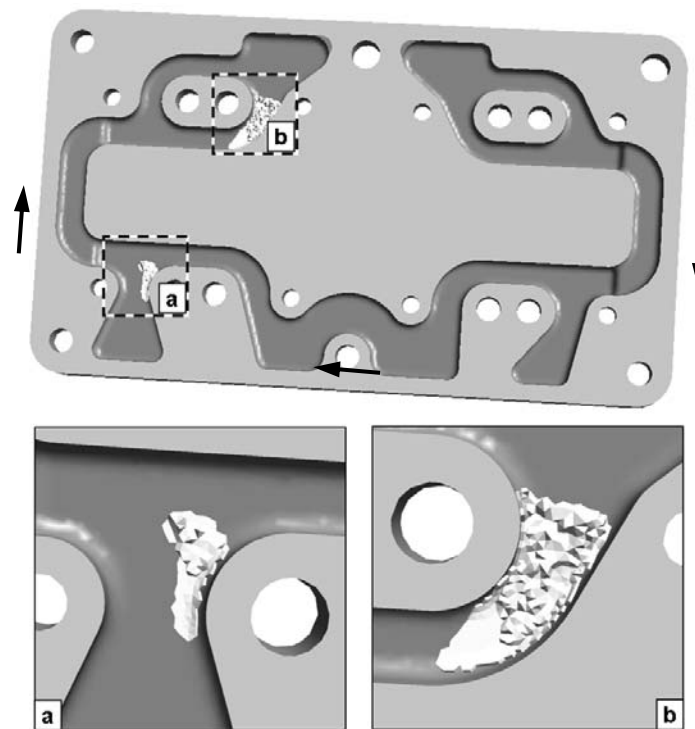


Figure 15. Iso-volumes of vapour: volume fraction above 0.01% is highlighted

The temperature of a cooled surface is basically dependent on the distribution of thermal load underneath, and the cooling efficiency above the surface, which could be both driven by part geometry. It is noticeable in Figure 14 and 15 that the occurrence of

steam propagation is not accompanying with peak heat flux as one would expect after investigating the *N-curve* of pool boiling in *Figure 2*. According to the simulation result, vapour is generated in the system where the wall temperature exceeds saturation point. These local maximums of wall temperature occur, where the structure is exposed to high temperature load, and the velocity pattern of coolant indicates stagnation of the fluid at the same time.

The highest volume fraction of steam is 0.3% within the investigated cooling system. This means that there is at least one cell in the fluid domain in which the void fraction reaches 0.3%. The fluid is not exposed to uniformly high wall temperature, rather local peaks occur. As a consequent of this, the fluid remains subcooled throughout its passage, and even if nucleate boiling evolves at some locations, void fraction immediately condensates after passing to a subcooled region.

## 7. Conclusions

A three dimensional CFD analyses coupled with RPI wall boiling model are completed for the water jacket of a reciprocating compressor. The main goal of the presented feasibility study is to determine the hot spots, evaporated regions, heat transfer characteristics of the jacket and to provide information about the applicability of the RPI wall boiling model of ANSYS CFX for vehicle industry applications in time, accuracy, capacity and cost point of view.

With adding boiling sub-models to the simulation the heat transfer is modelled more accurately, and hence the resulting temperature distributions on solids might be more realistic. The upper presented simulation model can expose steam phase propagation in its initial state. The pre-processing is 30 % more time consuming and the solver time is also increased. Convergence is highly sensitive to empirical sub-model parameters; furthermore some of the available sub-models are not really applicable to subcooled boiling [8].

Most of the recently available commercial CFD codes are developed to be able to receive user imposed commands. An input interface for user programmed add-ons is provided to tailor simulation in order to meet certain requirements. Boiling flow in a subcooled system is one of the situations where adjusted sub-models based on test bench measurements may provide more accurate result, but the validation process in industrial scale applications could be very expensive or even unaccomplishable. Other codes such as *Fluent* or *Relap5* for instance are also used commonly for investigating boiling systems.

Concluding all the above statements, it seems to be obvious that applying RPI wall boiling model of ANSYS CFX for such a subcooled system is only advised with strong experience. Maintaining velocity and pressure fields with CFD code by modelling the fluid volume only can provide information on any choked region, high pressure drop spots, separation bubbles and stagnation locations. With including solid bodies in the model, the entire energy mapping of the system can also be modelled in order to highlight critical zones of possible overheating. By adding the wall boiling model as well, on one hand the thermal phase change can be localized in its initial status while the thermal mapping of domains is getting more realistic, but on the other hand the RPI

model requires coarse boundary layer mesh resolution, so it makes the simulation inaccurate in terms of inertial and shear force analysis.

Further investigation should be completed by means other approaches implemented in *Fluent* environment for example or transient analyses.

### Acknowledgement

TAMOP-4.2.1/B-09/1/KONV-2010-0003: Mobility and Environment: Researches in the fields of motor vehicle industry, energetics and environment in the Middle- and West-Transdanubian Regions of Hungary.

The Project is supported by the European Union and co-financed by the European Regional Development Fund.

### References

- [1] Ghoshdastidar, P. S.: *Heat Transfer*, Oxford University Press, ISBN-10: 0195670507, ISBN-13: 978-0195670509, (2004).
- [2] Graham, R. W., Yih-Yun Hsu: *Transport Processes in Boiling and Two-Phase Systems*, Hemisphere Publishing Corporation, Washington, ISBN: 0-07-030637-0, (1976).
- [3] Sjoerd van Stralen, Cole, R.: *Boiling Phenomena*, McGraw-Hill Book Company (UK), Washington, ISBN: 0-07-067612-7, ISBN: 0-07-079189-9, (1979).
- [4] Stephan, K.: *Heat Transfer in Condensation and Boiling*, Springer-Verlag, Stuttgart, ISBN: 3-540-52203-4, (1992).
- [5] Ansys Hotline Support Team, England, (2010).
- [6] Kurul, N., Podowski, M. Z.: *On the modelling of multidimensional effects in boiling channels*, In Proceedings of the 27th National Heat Transfer Conference, Minneapolis, Minnesota, USA. (1991).
- [7] Lemmert, M., Chawla, L. M.: *Influence of flow velocity on surface boiling heat transfer coefficient*, in Hahne, E., Grigull, U., Eds.: *Heat Transfer in Boiling*, Academic Press and Hemisphere, New York, NY, USA., ISBN-10: 0123144507, ISBN-13: 978-0123144508, (1977).
- [8] Ansys 13.0 official help, (2010).
- [9] Hack, F., Kugler, S., Radnai, Gy., Tóth, G.: *Négyjegyű függvénytáblázatok matematikai, fizikai, kémiai összefüggések*, Tankönyvkiadó, Budapest, ISBN 9631808440, (1988).